Design of a distributed ultrasound-based sensory system

Jasmina Zubaca, Mina Ferizbegovic, Kenan Softic, Emir Sokic, Melita Ahic-Djokic
Department of Automatic Control and Electronics
Faculty of Electrical Engineering, University of Sarajevo
Sarajevo, Bosnia and Herzegovina
jzubaca1@etf.unsa.ba

***Abstract*—Different sensors may be used for a robot environment analysis: infrared sensors, laser sensors, sonars, RGB and depth cameras. Most of them provide satisfying information about the distance and the shape of observed objects. However, the main drawback of these sensors is the inability to discriminate among different analyzed objects if the latter share the same color, texture or distance. A distributed ultrasound-based sensory system composed from multiple ultrasonic cells is proposed. The system uses a master-slave control architecture. This paper presents the most important part of such system - a low-cost ultrasonic cell with the ability to classify objects by exploiting the magnitude of reflected ultrasonic waves. Traditional ultrasonic sensors only provide information about the distance, but the presented ultrasonic cell also measures the acoustic reflection coefficient of analyzed object. This coefficient allows to differ among materials or objects. Experiments are conducted to demonstrate the performance of the proposed ultrasonic cell.**

***Index Terms*—Ultrasound; Sensory system; Material; Obstacle; Reflection; Environment analysis; Distributed system**

I. Introduction

Environment analysis is one of the most significant problems in the field of autonomous robotic systems. It provides crucial information for motion control in an unknown environment. For example, in a simultaneous localization and mapping problem (SLAM), the information gathered from sensors are very important [1]. Applications of environment analysis can be found in different areas: from space exploration [2], via industrial manipulator [3] to medical surgery [4]. Most important applications of environment analysis are in the autonomous navigation of unmanned underwater, ground, or air vehicles. This type of analysis demands precise, reliable and informative measurements, which restricts the type of sensors that can be used.

An important factor when choosing a sensor is the price, especially if a large number of sensors are needed for measurement. Varieties of sensors are used for environment analysis, such as optical sensors (mainly infrared sensors), lasers, and cameras [5]. Each of these types of sensors have few disadvantages: optical sensors are sensitive to environmental conditions (such as light, rain, fog, etc.) [6], laser sensors are expensive and often demand large power supply [7], and RGB cameras provide excellent data for further image processing, but a single camera cannot provide information about distance of nearby objects [8].

Ultrasonic sensors, on the other hand, have satisfying precision and very good characteristics. They are also able to determine structure and solidity of materials and objects [9]. Different types of these sensors can be found, ranging from very inexpensive to extremely expensive specialized ultrasonic sensors. Besides their application in robotic systems, these sensors are used for flow measurements [10], fault detection for ships or aircrafts [11], and process monitoring [12].

The ability to discriminate among different types of materials and objects is from great importance for a robotic system. Traditional low-cost solutions based on ultrasonic sensors are not able to distinguish different materials. The aim of this work is to design simple, inexpensive, and distributed ultrasound-based sensory system. This system consists of multiple ultrasound-based sensor cells. Each cell is able to provide information about the nearby material and object, based on magnitude of reflected ultrasonic waves. The most important characteristic of this system is its ability to recognize different materials and objects, based on the reflected magnitude of ultrasonic waves.

A single ultrasonic cell can be used for environment analysis, but its sensing area is very narrow. A common approach is to place a single ultrasonic cell on a moving platform, but we propose to use a distributed sensory system, as illustrated in Figure 1. An array of multiple ultrasonic cells can provide information for a wider spatial area. A master device (PC or microcontroller) is used to control single cells, and to acquire data from these cells for further analysis and processing. A PC enables to merge information from RGB camera and other sensors with ultrasound extracted signals, hence acquiring a informational-rich environment assessment. Each ultrasonic cell will analyse one part of the environment and provide corresponding information, that are used to process a specific part of the image from the camera. This approach enables to obtain a structural image of the environment, as depicted in Figure 2. Therefore, different objects may be differentiated according to their structure instead of color or position.

In this paper, we will mostly focus on presenting the design and implementation of the slave ultrasonic cell. Experimental results proved that proposed sensory cell can be used in prac-

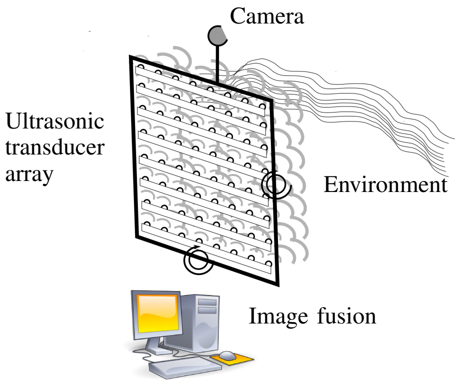

Figure 1. A simplified sketch of the proposed distributed sensory system

Figure 2. Left: original image; Right: one of the possible representations of a fused "structural" image - different materials are shaded with different grayscale tones.

tical applications to differ nearby objects and materials. The details on the master control system, image fusion algorithms and the corresponding experimental results are omitted from this paper due to the space limit, and they are considered to be the part of a future work.

The paper is organized as follows. Section II describes the theoretical foundations of our sensory system. The proposed design of the system and the implementation of a single ultrasonic cell are given in Section III, while the experimental results are presented in Section IV. Conclusion, alongside with future plans, are given in the last section.

II. Principles of Operation

A. Distance computation

Ultrasonic transceiver emits sound waves which propagate in the air at the velocity of sound. If they strike an obstacle, they are reflected back as echo signals. The time-span between the emission of the sound wave and the receiving echo is used to determine distance to an obstacle:

$$d = \frac{1}{2}ct, \tag{1}$$

where c is velocity of sound in air. Due to the influence of the temperature, pressure and humidity, sound velocity is changed. By neglecting pressure and humidity variations, sound velocity may be computed using [13]:

$$c = 331.4 + 0.6T, \tag{2}$$

where T is the ambient air temperature.

B. Material discrimination

In order to discriminate among materials or objects, the difference between the magnitudes of transmitted and received ultrasonic waves need to be analyzed. Usually, the behavior of sound waves in air can be analytically described using the lossless wave equation [14]. Due to the high frequency of the ultrasound, the attenuation in the air should also be taken into account. In addition, the sound wave reflected to the transceiver is attenuated because of the absorption on the obstacle itself. In order to describe this phenomenon, one should start with a more general form of the non-linear Navier-Stokes equation [15], [16], given with:

$$\rho\left(\frac{\partial\overrightarrow{u}}{\partial t} + (\overrightarrow{u}\cdot\nabla)\overrightarrow{u}\right) = -\nabla p + \left(\frac{4}{3}\eta + \eta_B\right)\nabla(\nabla\cdot\overrightarrow{u}) - \eta\nabla\times\nabla\times\overrightarrow{u}, \tag{3}$$

where $\overrightarrow{u}$ represents particle velocity, ρ fluid density, η and η_B are coefficients of shear and bulk viscosity respectively. After the linearization of the left side of the equation (3), using the linearized equation of continuity and the adiabatic assumption it simplifies to the lossy wave equation:

$$\left(1 + \tau_s\frac{\partial}{\partial t}\right)\nabla^2 p - \frac{1}{c^2}\frac{\partial^2 p}{\partial t^2} = 0, \tag{4}$$

where p is acoustic pressure, τ_s represents the relaxation time, and c is the thermodynamic velocity of sound. If monofrequency motion $e^{j\omega t}$ is assumed, where ω is sound's frequency, then the relation (4) simplifies to the lossy Helmholtz equation ($\nabla^2\mathbf{p} + \mathbf{k^2 p} = 0$, where $\mathbf{k} = k - j\alpha$), whose solution is given with:

$$\mathbf{p} = P_0 e^{-\alpha x} e^{j(\omega t - kx)}. \tag{5}$$

The complete derivation of the relation (5) is not presented in this paper for brevity (see e.g. [15] for more details).

As it may be seen from solution (5), the sound pressure magnitude decreases exponentially with distance traveled. One of the common simplifications for computing the attenuation rate α [16] is the famous Stokes' Law, which states that the amplitude of a plane wave decreases at a rate which is given by:

$$\alpha = \frac{2\eta\omega^2}{3\rho c^3}, \tag{6}$$

where η is the dynamic viscosity coefficient of the fluid, ρ is fluid density and c is the speed of sound in the medium. The coefficient α (given in $[Np/m]$), which is commonly referred to as the spatial absorption coefficient, may have different forms [17]. Commonly, the coefficient α is governed by a power law, and different forms are proposed for different type of media and sound signals (e.g. [18], [19]). Taking into account that the proposed system will be used in a specific experimental setup (constant sound frequency and medium) according to the experimental results presented in the work [20], it can be concluded that sound attenuation absorption coefficient can be considered as a constant.

The second part of sound attenuation is caused by the absorption on the obstacle. When a wave reaches a boundary, a part of it will be reflected and a part transmitted through the boundary. The sound pressure reflection coefficient R is defined as the ratio of the magnitude of the reflected wave to that of the incident wave created by the obstacle. Different materials have different reflection coefficients. Density of material, sound velocity in the air and the material, and the incidence angle are main parameters which affect the reflection coefficient.

The incident wave, reflected wave, and transmitted wave must obey two boundary conditions: continuity of pressure (the acoustic pressure must be the same on both sides of the boundary) and continuity of normal particle velocity (particle velocities normal to the boundaries must be equal). Using these conditions, it can be easily derived (see e.g. [21]) that pressure reflection coefficient may be computed using:

$$R = \frac{mcos\theta - ncos\theta_1}{mcos\theta + ncos\theta_1}, \tag{7}$$

where $m = \rho_1/\rho$, $n = c/c_1$, and the densities and sound speeds in the air and inspected material are ρ, c and ρ_1, c_1 respectively. Initially, we consider only the normal incidence $\theta = \theta_1 = 0$. It is clear that the type of the material may be determined if the magnitudes of the transmitted and received waves are compared. Therefore, if the magnitude of the incident wave at the boundary prior to reflection from the obstacle at distance d is assumed $A_0 e^{-\alpha d}$ (A_0 is the magnitude of the wave at the source), then the magnitude of the reflected wave next to the boundary is $A_0 R e^{-\alpha d}$. Therefore, for different obstacles placed at the same distance, the magnitudes of the reflected sound waves are distinct. To this end, a simplified model of the measured reflected signal magnitude is given by the following equation:

$$\begin{aligned} A_r &= \underbrace{A_0}_{initial} \cdot \underbrace{e^{-\alpha d}}_{travel} \cdot \underbrace{R}_{reflection} \cdot \underbrace{e^{-\alpha d}}_{travel}, && (8) \\ &= A_0 \cdot R \cdot e^{-2\alpha d}, && (9) \\ &= A_0 \cdot R \cdot 10^{-B \cdot 2 \cdot d/10}, && (10) \\ \Rightarrow\ & R = \frac{A_r}{A_0} 10^{B \cdot 2 \cdot d/10}, && (11) \end{aligned}$$

where A_r and A_0 are the magnitudes of the reflected and transmitted waves respectively, R is the reflection coefficient of the material, d is the distance between the obstacle and the ultrasonic sensor and B represents the attenuation of the ultrasonic wave in the air. It is important to note that B is converted to $[dB/m]$ for convenience. Moreover, B includes the losses induced by voltage-sound conversion, and it is dependent on temperature, pressure and humidity [20]. The value of the coefficient B was empirically determined as $2.4[dB/m]$ for our setup.

III. The Proposed System

The structure of the proposed system is given in Figure 3. It consists of N master cells connected to a PC, and each master cell controls M (up to eight) slave ultrasonic cells.

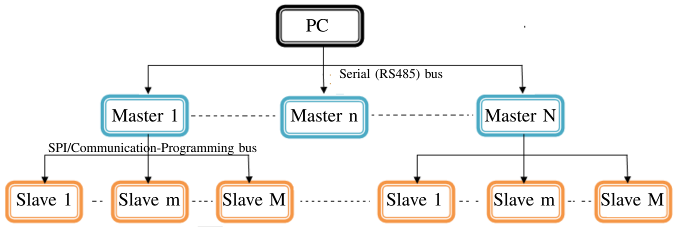

Figure 3. Block diagram of the proposed system.

A. Ultrasonic cell

A simplified diagram of a single ultrasonic cell is presented in Figure 4. Instead of commonly used two piezoelectric ultrasonic transceivers to transmit and receive ultrasound waves, the proposed ultrasonic cell consists of only one transceiver.

1) Hardware design: Conceptual prototype of this ultrasound-based sensory system is created from eight individual ultrasonic cells, which are connected to one master device (PC or microcontroller). Master device gathers information obtained from ultrasonic sensor, controls individual units, and sends obtained data to PC for further processing. Ultrasonic cell includes ultrasonic sensor used for producing and acquiring ultrasound, which is managed by a microcontroller unit (MCU). Cell also includes a section for amplification of the acquired ultrasonic signal, a section for communication, a demodulating section, a section for voltage regulator, and a temperature measurement section. The ultrasonic cell circuit diagram is depicted in Figure 5. Explanations for every section are given below.

Ultrasonic sensor: Ultrasonic sensor UTT4016 with central frequency of $40[kHz]$ is used. An important feature is that the same sensor is used as transmitter and receiver, instead of pair of sensors. This reduces the complexity of the cell and the number of the needed sensors by half. Other benefits of this sensor are low cost and narrow frequency with a bandwidth of $2[kHz]$.

Microcontroller unit (MCU): A reasonable choice for MCU is 8-bit Atmel ATMega 328P, because of its generally known advantages and characteristics, such as low cost, many analog inputs, possibility of using different types of communication, etc. The main task of the MCU is to produce the control signals for the ultrasonic sensor, and acquire signals from the ultrasonic sensor. Moreover, MCU is also used for simple processing of ultrasonic signals, communication with the master device (PC or other microcontroller), temperature compensation, etc. The MCU is clocked by a $16[MHz]$ quartz crystal, and powered by $5[V]$ voltage level.

Amplifier unit: Ultrasonic signals need amplification, which is realized by one two-stage amplifier, based on TL082 operational amplifier, as shown in Figure 5. Output amplifier is realized with bipolar transistors.

Demodulator unit: MCU uses an AD converter with sample rate of $6[kHz]$, while the signal from ultrasonic sensor has the frequency of $40[kHz]$ (with the bandwidth of $2[kHz]$). It is clear that direct sampling of ultrasonic signal would violate the Nyquist-Shannon sampling theorem. Therefore, the acquired

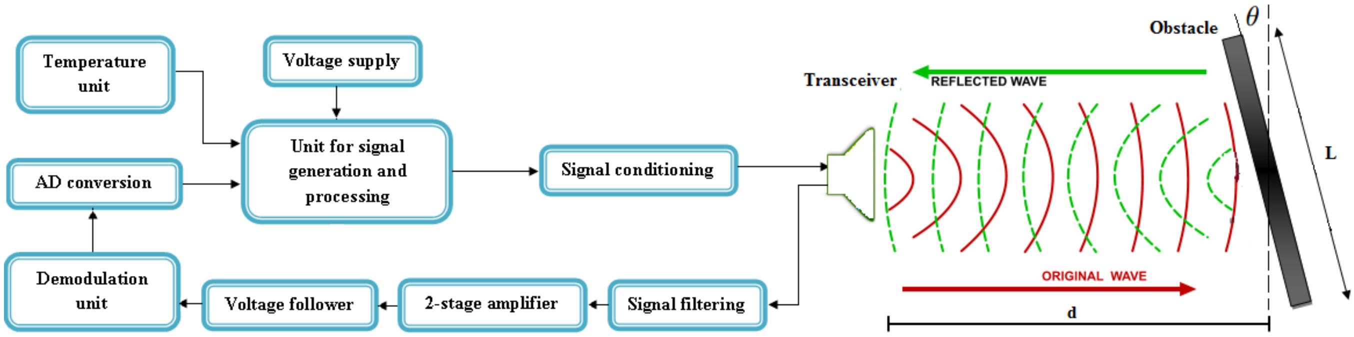

Figure 4. Block diagram of a single ultrasonic cell.

ultrasound signal is demodulated prior to sampling and A/D conversion. The demodulation circuit is shown in Figure 5, and it can be noticed that it is actually based on a rectifier and a low-pass filter.

Communication unit: The SPI protocol is used for communication, which enables easy communication of the master unit with multiple slaves. Also, this allows programming of multiple MCUs at the same time. Ultrasonic cell is equipped with RJ-45 connector, which provides pins used for SPI communication and the voltage needed for supplying the ultrasonic sensor. Moreover, the ultrasonic cell has an ICSP header, which allows in-circuit programming with commercial programmers.

Voltage regulation unit: Ultrasonic sensor is supplied by a bipolar $15[V]$ voltage source. Voltage of $5[V]$ is required for MCU, so an additional voltage regulator LM7805 is used.

Temperature measurement unit: Equation (2) is used to determine the speed of the ultrasound, by measuring the temperature of the environment. Therefore, temperature sensor KTY-81 was used for temperature compensation.

2) Signal generation and processing: The proposed system is able to measure the distance and magnitude of the reflected waves by using specific signals produced by MCU. These signals are shown in Figure 6.

The transmitting signal consists of short square wave bursts with $40[kHz]$ frequency and duration of $0.5[ms]$. MCU can generate these bursts independently or by command from a master device. Due to the fact that the transceiver acts as a bandpass filter, only the first harmonic of the periodic square wave signal is emitted into the air, therefore the transmitted signal is actually a sine wave. In order to measure distance up to $3[m]$ bursts are repeated in time periods larger than $20[ms]$ (max. refresh rate is $50[Hz]$), while in order to prevent the interaction of the transmitted and received sound wave for shorter distances the burst had to be shorter than $0.5[ms]$. Due to these time limitations, the transceiver may be used as transmitter and receiver simultaneously.

The reflected waves are $40[kHz]$ modulated sine waves. Magnitude of the reflected waves determines the reflection coefficient of the obstacle. However, sampling the reflected signal directly with a low frequency would violate the Nyquist-Shannon theorem and would not provide a satisfying accuracy

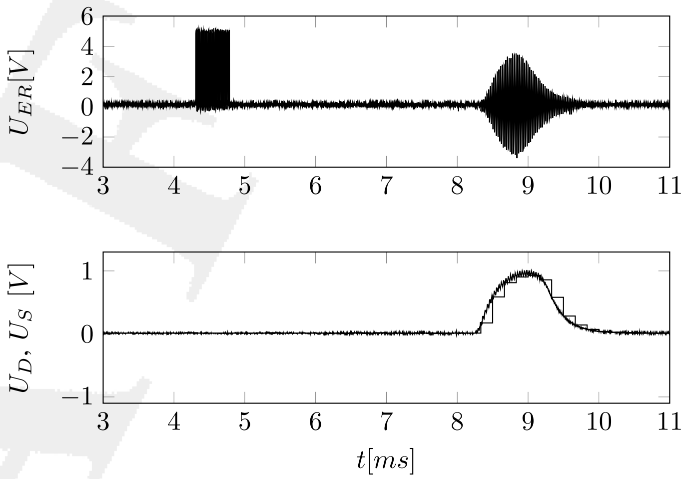

Figure 6. Signal generated and received by the transceiver (U_{ER}), the demodulated signal (U_D) and sampled demodulated signal (U_S) processed by the MCU. Note that time and magnitude scale were slightly changed for a more convenient presentation of the signals.

of the reflected wave magnitude estimation. In order to sample the signal with a non-expensive MCU, the reflected signal first needs to be demodulated. After demodulation, a truncated Whittaker-Shannon-Kotelnikov series is used for magnitude estimation:

$$\widetilde{U}_D(t) = \sum_{k=-N}^{N} U_S\,(kT)\,sinc(2\omega_C(t-kT)), \qquad (12)$$

where $sinc(t) = sint/t$ for $t \neq 0$ and $sinc(0) = 1$, $2N+1$ is the number of samples, T is the sample period, and ω_C is the bandlimit of the demodulated signal. Series given by (12) converges absolutely and uniformly on $\mathbf{R}$ if $N \to \infty$ [22]. In the performed experiments, a value of $N = 50$ has been used, which resulted in the maximal error of 5.6% over the full scale range.

B. Master device

The main purpose of the master units is to facilitate sending and receiving data from multiple slave cells as well as from

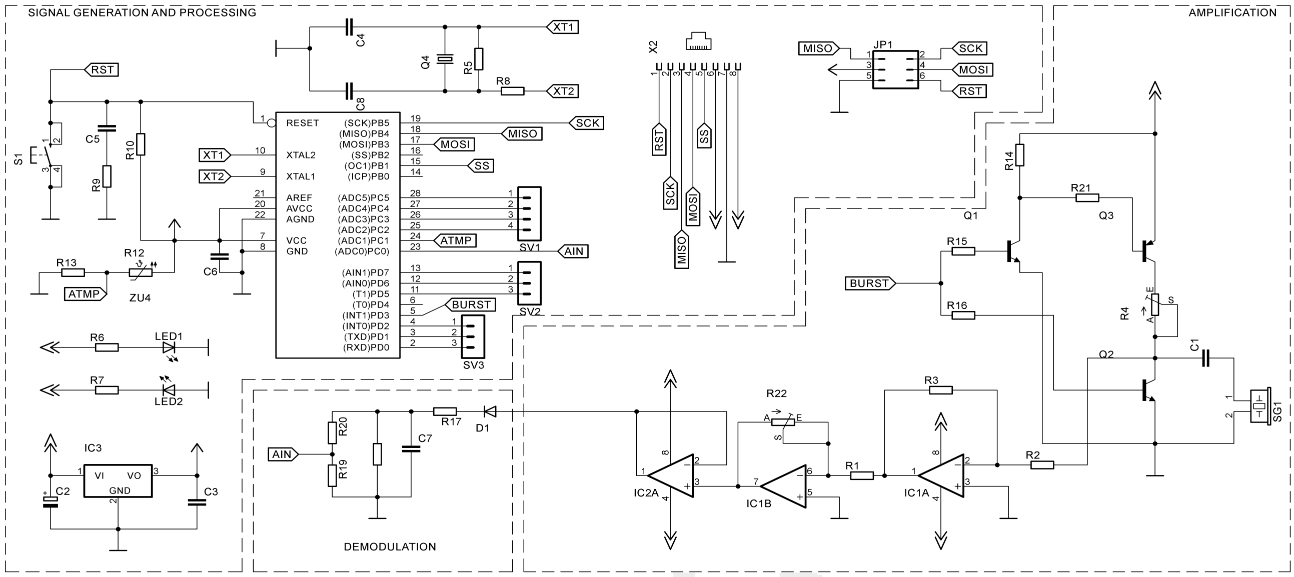

Figure 5. Circuit diagram of the proposed ultrasonic cell.

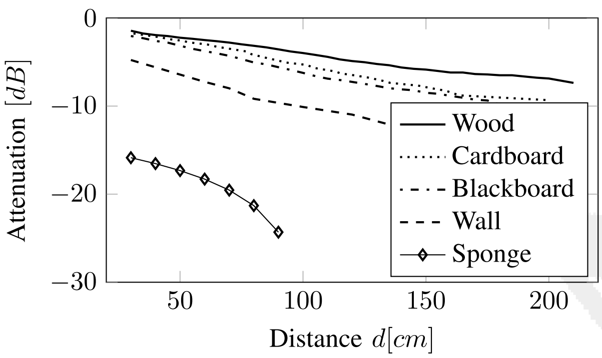

Figure 7. Attenuation of the sound over different obstacles at distance d.

the PC. A master can excite an ultrasonic cell and read useful information, such as the obstacle's distance, or reflection coefficient. Two different types of communication are used; serial (RS485 based) communication is used to communicate with the PC, while SPI communication is used to communicate and program slave cells. Master units are based on the ATMega 1280 microcontroller with multiple communication and control pins.

Since every slave cell has its own simple signal preprocessing algorithm, it is necessary to have the possibility to change the corresponding firmware. Although each ultrasonic cell posses an ICSP header and it can be programmed independently, master units are also used as automatic programmators. They have the possibility to program several ultrasonic units simultaneously using the PC, thus the amount of time needed for programming is significantly reduced.

IV. Experimental results

Five obstacles of various sizes made from different materials have been used as a test set in the performed experiments: wood, cardboard, blackboard, wall and sponge. Each type of obstacle has a different absorption coefficient, therefore the measured reflected sound signal is attenuated differently for every material. The experimentally obtained attenuation of a sound wave as a function of distance for each material is depicted in Figure 7.

The nominal reflection coefficient R for different materials may be determined from (11), the estimated reflected wave magnitude A_r and distance d. The reflection coefficients have been experimentally determined using 86 independent measurements (eighty percents of all conducted measurements), for different materials at various distances. Due to measurement errors and noise, nominal coefficients R can be computed only with a certain tolerance. Therefore, all computed values of coefficients were fitted by a normal (Gaussian) probability distribution centered around expected value of coefficient R, as shown in Figure 9. The fitting was achieved using MATLAB programming environment.

The rest of the 20% of the measurements was used to investigate the classification abilities of the proposed ultrasound unit. The classification of unknown obstacles was conducted using 1-nearest neighbor classifier. The extracted mean values of the reflection coefficients for different materials are used as inputs to the classifier. The classifier made correct classification in 89.47% of cases.

Moreover, experiments showed other interesting results. The standard deviation of the magnitude estimation with fixed distance and surface using equation (12) is only $0.055[V]$. The standard deviation was computed using one minute of continuous measurement (50 samples per second). The measurements are not significantly influenced by the dimensions of the obstacle, which becomes noticeable only if the obstacle dimensions are under $0.1d$. The frequency response of the ultrasonic cell and its directional characteristic are experimentally determined, and are depicted in Figure 8.

The main drawback of the ultrasonic cell is probably its

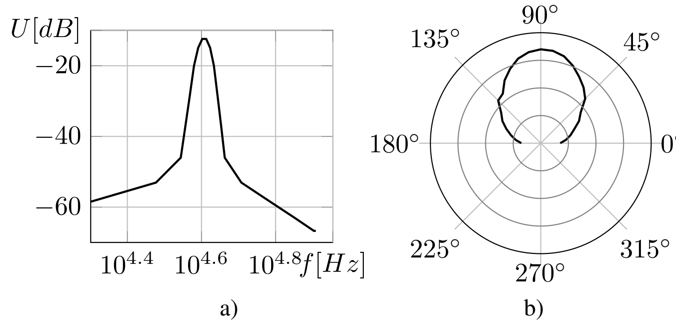

Figure 8. a) Frequency response, b) directional characteristic of the ultrasonic cell.

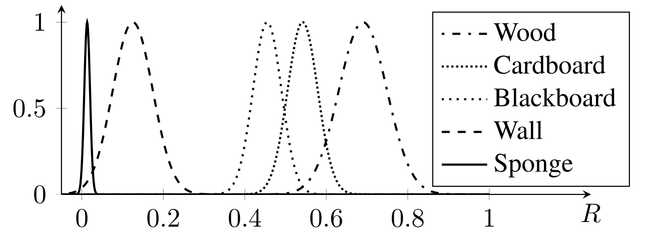

Figure 9. The dispersion of the reflection coefficient R for different materials.

directivity. Since the sensor is very directional, a standalone ultrasonic cell works as expected only if the surface is nearly perpendicular to the sound path. It is found experimentally that inclination angle for which the system works properly is 6 degrees. For values that are out of defined range, magnitude decreases almost linearly as inclination angle increases. This means that dependence on the inclination angle needs to be eliminated in future designs. We propose to combine distance and magnitude measurements from at least three spatially distributed ultrasonic cells, so that the inclination angle of the surface may be estimated, hence the magnitude values may be compensated for non-perpendicular surfaces.

V. Conclusion and guidelines for future work

In this paper we presented the design and implementation of a low-cost ultrasonic cell, as a part of a larger ultrasound-based distributed sensory system, used for classification of obstacles and objects. Experimental results demonstrated promising performance of such ultrasonic cells, and their possible usage of in tasks of environment analysis.

As a part of a future work, the overall performance of a master-slave based sensory architecture will be investigated. This will enable the usage of very large number ultrasonic cells, and facilitate the environment analysis of a larger area. Once the system is fully developed, we plan to combine readings from this distributed sensory system with other sensors (RGB camera, Kinect, laser), to form hybrid 2D and 3D structural images.

Acknowledgment

This paper is published as part of the project “A hybrid 2D visualization of the environment using ultrasonic reflections”, funded by the Federal Ministry of Education and Science Bosnia and Herzegovina.

References

[1] J. Fuentes-Pacheco, J. Ruiz-Ascencio, and J. M. Rendón-Mancha, “Visual simultaneous localization and mapping: a survey,” *Artificial Intelligence Review*, vol. 43, no. 1, pp. 55–81, 2015.

[2] A. Elfes, J. M. Dolan, G. Podnar, S. Mau, and B. Marcel, “On generating the motion of industrial robot manipulators,” *Safe and efficient robotic space exploration with tele-supervised autonomous robots*, vol. 1, pp. 104–113, 2006.

[3] K. Kaltsoukalas, S. Makris, and G. Chryssolouris, “On generating the motion of industrial robot manipulators,” *Robotics and Computer-Integrated Manufacturing*, vol. 32, pp. 65–71, 2015.

[4] P. Mountney, D. Stoyanov, A. Davison, and G.-Z. Yang, “Simultaneous stereoscope localization and soft-tissue mapping for minimal invasive surgery,” *Medical Image Computing and Computer-Assisted Intervention – MICCAI*, vol. 1, pp. 363–371, 2008.

[5] J. Aulinas, Y. Pettilot, J. Salvi, and X. Lladog, “The slam problem: a survey,” *Artificial Intelligence Research and Development*, vol. 1, pp. 347–354, 2006.

[6] G. Benet, F. Blanes, J. E. Simó, and P. Pérez, “Using infrared sensors for distance measurement in mobile robots,” *Robotics and autonomous systems*, vol. 40, no. 4, pp. 255–266, 2002.

[7] H. G. Jung, Y. H. Cho, P. J. Yoon, and J. Kim, “Scanning laser radar-based target position designation for parking aid system,” *Intelligent Transportation Systems, IEEE Transactions on*, vol. 9, no. 3, pp. 406–424, 2008.

[8] I. Fernández, M. Mazo, J. L. Lázaro, D. Pizarro, E. Santiso, P. Martín, and C. Losada, “Guidance of a mobile robot using an array of static cameras located in the environment,” *Autonomous Robots*, vol. 23, no. 4, pp. 305–324, 2007.

[9] S. Grzelak, J. Czoków, M. Kowalski, and M. Zieliński, “Ultrasonic flow measurement with high resolution,” *Metrology and Measurement Systems*, vol. 21, no. 2, pp. 305–316, 2014.

[10] X. Han, J. Wang, Z. Peng, and J. Zhang, “A study of ultrasonic flowmeter in ship piping leakage detection system,” *Intelligent Systems and applications (ISA)*, vol. 1, pp. 769–773, 2011.

[11] J. D. Champaigne, Kevin andSumners, “Low-power electronics for distributed impact detection and piezoelectric sensor applications,” *Aerospace Conference*, vol. 9, pp. 3911–3919, 2007.

[12] D.-H. Kim, B.-S. Yang, and S.-B. Lee, “3d boiler tube leak detection technique using acoustic emission signals for power plant structure health monitoring,” *Prognostics and System Health Management Conference*, vol. 1, pp. 256–263, 2011.

[13] G. S. Wong, “Speed of sound in standard air,” *The Journal of the Acoustical Society of America*, vol. 79, no. 5, pp. 1359–1366, 1986.

[14] R. P. Feynman, R. B. Leighton, and M. Sands, *The Feynman Lectures on Physics, Desktop Edition Volume I.* Basic Books, 2013, vol. 1.

[15] L. E. Kinsler, A. R. Frey, A. B. Coppens, and J. V. Sanders, “Fundamentals of acoustics,” *Fundamentals of Acoustics, 4th Edition, by Lawrence E. Kinsler, Austin R. Frey, Alan B. Coppens, James V. Sanders, pp. 560. ISBN 0-471-84789-5. Wiley-VCH, December 1999.*, vol. 1, 1999.

[16] A. S. Dukhin and P. J. Goetz, *Characterization of liquids, nano-and microparticulates, and porous bodies using ultrasound.* Elsevier, 2010, vol. 24.

[17] P. Straka, M. Meerschaert, R. McGough, and Y. Zhou, “Fractional wave equations with attenuation,” *Fractional Calculus and Applied Analysis*, vol. 16, no. 1, pp. 262–272, 2013.

[18] M. Caputo, “Linear models of dissipation whose q is almost frequency independent-ii,” *Geophysical Journal International*, vol. 13, no. 5, pp. 529–539, 1967.

[19] T. L. Szabo, “Causal theories and data for acoustic attenuation obeying a frequency power law,” *The Journal of the Acoustical Society of America*, vol. 97, no. 1, pp. 14–24, 1995.

[20] A. Vladišauskas and L. Jakevičius, “Absorption of ultrasonic waves in air,” *Ultragarsas*, vol. 1, p. 50, 2004.

[21] B. Cox, “Acoustics for ultrasound imaging,” *Lecture Notes, University College London*, 2012.

[22] P.-x. Ye and Z.-j. Song, “Truncation and aliasing errors for Whittaker-Kotelnikov-Shannon sampling expansion,” *Applied Mathematics-A Journal of Chinese Universities*, vol. 27, no. 4, pp. 412–418, 2012.

[23] D. Vray, E. Brusseau, V. Detti, F. Varray, A. Basarab, O. Beuf, O. Basset, C. Cachard, H. Liebgott, and P. Delachartre, “Ultrasound medical imaging,” *Medical Imaging Based on Magnetic Fields and Ultrasounds*, pp. 1–72, 2014.